

RHEOLOGICAL PROPERTIES OF SALICYL-IMINE-CHITOSAN HYDROGELS: EFFECT OF CROSSLINKING DENSITY

MANUELA-MARIA IFTIME and SIMONA MORARIU

“Petru Poni” Institute of Macromolecular Chemistry, 41A, Grigore Ghica Voda Alley,
700487 Iasi, Romania

✉ Corresponding author: S. Morariu, smorariu@icmpp.ro

Received June 20, 2022

The present paper focuses on the rheological behaviour of a series of hydrogels prepared from chitosan and salicylaldehyde. The unusual crosslinking of chitosan with this monoaldehyde was assessed by ^1H NMR spectroscopy, which demonstrated the formation of covalent imine bonds. The hydrogels exhibited a super-porous morphology, evidenced by SEM measurements, and the layered supramolecular structure of the hydrogels was sustained by the birefringence texture of the hydrogels, observed by polarized light microscopy (POM). The hydrogel-like behaviour was confirmed by rheologic measurements for the sample containing the highest salicylaldehyde amount. The dynamic flow properties of salicyl-imine-chitosan hydrogels with different crosslinking degrees (NH_2/CHO ratios between 2 and 4) were investigated at temperatures in the range of 20–40 °C. The rheological moduli were determined over a wide range of oscillatory frequencies and the experimental results were presented using master curves. In addition, the thixotropic behaviour of the hydrogels based on chitosan and salicylaldehyde was determined and discussed. The measurements of thixotropy were performed by increasing the shear rate to 400 s^{-1} in an upward sweep, followed by its decreasing in a downward sweep. It was noticed that the thixotropy of hydrogels increases with an increasing crosslinking degree. In line with this rheological behaviour, the self-healing ability was tested, and it was proved that the hydrogels were able to reshape after applying deformation stress.

Keywords: chitosan, hydrogel, rheology, thixotropy, self-healing

INTRODUCTION

In recent years, chitosan hydrogels have received special attention due to their versatile properties (biodegradability, biocompatibility, non-toxicity, ability to swell and absorb different active compounds) and their applicability in various fields of biomedicine and agriculture.¹⁻⁴

The inclusion of chitosan into composites or hydrogels provides them with new functional properties for different applications. Usually, chitosan is chemically crosslinked by acid condensation of the functional amine groups with dialdehydes forming imine bonds, but the applicability of the obtained materials in the biomedical field is limited because of the toxicity of dialdehydes. Hydrogels based on chitosan have been prepared by using various dialdehydes as crosslinking agents: glutaraldehyde,⁵ genipin,⁶ tannic acid⁷ etc. Chitosan hydrogels with enhanced elasticity under physiological conditions, suitable for the encapsulation of cells and bioactive molecules, were obtained by using

genipin as crosslinking agent.⁶ Genipin is preferred as chemical crosslinker because it is a natural compound, with low toxicity. Research on the rheological properties of the hydrogels obtained by crosslinking with genipin revealed that hydrogels with a weak structure, suitable for application in food processing, can be prepared from chitosan with a deacetylation degree of 96%.⁸ The gelation temperature decreased with the increase of deacetylation degree. Thereby, chitosan with deacetylation degrees of 83%, 94% and 96% (chitosan concentration in an initial solution of 3%) exhibited sol-gel transition temperature at 75 °C, 30 °C and 25 °C, respectively.

Our previous papers reported the preparation of chitosan hydrogels with good mechanical properties and thixotropic behaviour, appropriate for biomedical applications, by using a monoaldehyde as crosslinking agent: salicylaldehyde,⁹ cinnamaldehyde,¹⁰ 2-

formylphenylboronic acid,^{11,12} pyridoxal 5-phosphate¹³ and citral.¹⁴ It was demonstrated that the formation of chitosan hydrogels using a monoaldehyde implies the self-assembling of the imino-chitosan chains in a three-dimensional architecture.

3D porous structures based on chitosan were prepared by Michael addition reaction between thiol modified chitosan and bismaleimide.¹⁵ This method, characterized by gentle reaction conditions and high regioselectivity, allowed obtaining hydrogels based on chitosan with improved storage modulus. By controlling the crosslinker amount, hydrogels with rheological and swelling properties targeted for biomedical applications can be obtained.

The freeze/thawing or freeze-drying techniques were frequently used for the preparation of physical hydrogels based on chitosan. The poly(vinylpyrrolidone)/chitosan hydrogel (50/50) obtained by the freeze-drying method revealed the best release of tetracycline hydrochloride, proving to be a good candidate for pharmaceutical formulations.¹⁶ Physically crosslinked chitosan hydrogels with optimal rheological properties for application in regenerative medicine were obtained by changing the pH value, by using a gelation temperature of 4 °C and higher chitosan concentrations in the initial solution (1.5% or 2%).¹⁷

Physical sodium alginate/chitosan hydrogels loaded with Nystatin were obtained by mixing solutions of the two polymers and the drug, followed by a coacervation procedure in 2-propanol.¹⁸ The rheological measurements proved that an increase in the chitosan amount in the hydrogel determined an increase in network density and an enhancement of gel strength. The optimum sodium alginate/chitosan ratio to obtain hydrogels suitable for mucosal application of Nystatin was estimated at 60/40 (v/v%). Fragile alginate/chitosan hydrogels (suitable for citral encapsulation and delivery) were obtained at basic pH, while a tough and more elastic composite was prepared at acid pH.¹⁹ The increase in the chitosan amount in the composite hydrogels induced a decline in their strength at acidic pH and at basic pH, weaker hydrogels being obtained with higher amounts of alginate. High viscoelasticity and maximum encapsulation capacity were noticed for hydrogels prepared at neutral pH. Xanthan/chitosan hydrogels with encapsulated Neomycin sulphate are suitable for

cosmetic applications (creams and ointments) due to their consistency.²⁰ The dynamic moduli values of xanthan/chitosan hydrogels with encapsulated Neomycin sulphate decrease with an increasing drug concentration, leading to smooth, soft and easily spreadable gels.

Chitosan scaffolds based on methoxypolyethylene glycol (mPEG) -aldehyde or -acetic acid were prepared by a crosslinking–cryogelation procedure, in which the –CHO and –COOH groups from PEG derivatives interact with the –NH₂ groups of chitosan.²¹ The mechanical properties of these scaffolds are not affected by the functionalization of mPEG, which influences only the network strength, important in the process of drug delivery. The cryogenic treatment was also used for preparation of chitosan/poly(vinyl alcohol) hydrogels, with applicability potential as injectable materials in the medical field.²² The number of freezing/thawing cycles necessary to obtain the sol–gel transition at 37 °C depends on the polymer total concentration in the initial mixture: for 3% and 10% polymer in the initial mixture, at least three and two freeze/thaw cycles, respectively, are required.

Bio-adsorbent hydrogels for Nigrosin acid dye from water were obtained by γ -irradiation grafting of acrylamide onto chitosan chains.²³ The optimal pH and chitosan/acrylamide ratio to obtain the maximum adsorption capacity were estimated at pH = 2 and 1/10 (wt/wt%).

Hybrid biocomposites based on natural/synthetic polymers and clay have attracted the attention of researchers due to their unique physical, chemical and biological properties as a result of combining the characteristics of each component. Chitosan/poly(ethylene oxide)/Laponite® RD hydrogels with enhanced viscoelastic properties were obtained due to the multiple interactions that can develop in the system: chitosan-chitosan, chitosan-clay platelets, poly(ethylene oxide)-clay platelets, chitosan-free or adsorbed poly(ethylene oxide) chains.²⁴ Chitosan/montmorillonite biocomposites with exfoliated structure were prepared by mixing the solutions of the components, followed by drying.²⁵ The antimicrobial activity of the composites containing clay was better than that of chitosan. In addition, the thermal stability of chitosan/montmorillonite composites enhances by increasing the added clay amount. Chitosan/poly(vinyl alcohol)/layered double

hydroxide biocomposites exhibited the best viscoelastic parameters at 37 °C around neutral pH, when the conditions to form the network structure are optimal.^{26,27}

In light of these data, the aim of the present paper was to study the rheological properties of a series of chitosan hydrogels obtained by crosslinking with various amounts of salicylaldehyde (SA). Special attention was dedicated to the investigation of their thixotropy in correlation with the self-healing behaviour proved by visual assesment.

EXPERIMENTAL

Materials

Low molecular weight chitosan (263 kDa, DA = 83%), salicylaldehyde (SA), ethanol and glacial acetic acid were provided by Sigma–Aldrich Co. (USA) and were used as received.

Preparation of chitosan hydrogels

Five hydrogels with different crosslinking degrees were obtained by acid condensation reaction of the chitosan with salicylaldehyde, according to a previously reported procedure (Scheme 1).⁹ The ratio between NH₂ and CHO groups (NH₂/CHO) of chitosan and SA used in the hydrogel preparation was varied from 2/1 up to 4/1. The hydrogels were denoted as Cx, where x represents the NH₂/CHO ratio (Table 1).

Characterization of hydrogels

Structural analysis was performed at room temperature by proton nuclear magnetic resonance (¹H NMR) in deuterated water as solvent, using a Bruker Avance DRX400 MHz Spectrometer (Billerica, MA, USA). The morphology was examined on the cross-section of the xerogels with a Scanning Electron Microscope SEM EDAX – Quanta 200 (SEM) (FEI, Brno, Czech Republic), operated at 20 kV accelerating voltage. The structural and morphological analysis was performed on samples frozen in liquid nitrogen and then lyophilized for 24 h, at –54 °C, by using a LABCONCO FreeZone Freeze Dry System (Kansas City, MO, USA).

The texture of the samples was investigated by polarized light microscopy using a Zeiss Axio Imager.A2m (Carl Zeiss AG, Oberkochen, Germany) microscope, provided with an Axiocam 208cc camera. The microscopy study was realized on thin slices of xerogels.

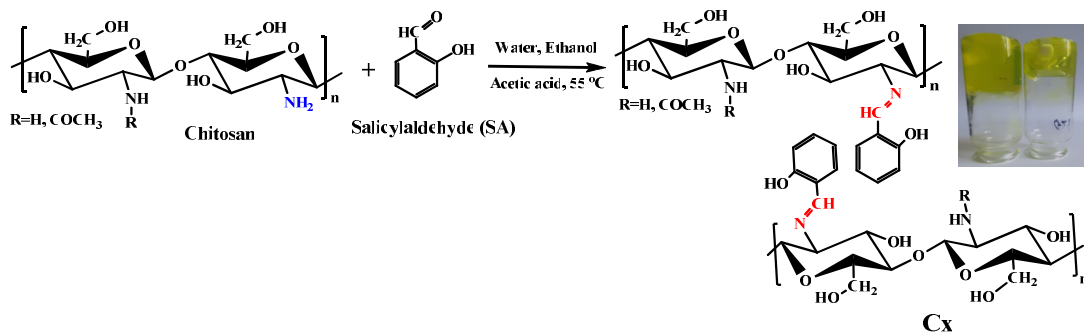
Rheological tests were carried out at various temperatures between 20 °C and 40 °C, by using an MCR302 Anton-Paar rheometer with plane-plane geometry (50 mm diameter). The thermal control and the evaporation limitation are assured by a Peltier device and an anti-evaporation device, respectively. The frequency sweep tests were performed at different temperatures in the frequency range of 3x10⁻¹–2x10² rad·s⁻¹, at a strain amplitude of 5% from the the linear viscoelastic regime, where the storage (G') and the loss (G'') moduli are frequency independent. The thixotropy was investigated from the hysteresis loop obtained by increasing the shear rate, $\dot{\gamma}$, from 2 s⁻¹ to 400 s⁻¹, keeping for 10 s at 400 s⁻¹, and decreasing $\dot{\gamma}$ to 2 s⁻¹ with a waiting time for each measured point of 5 s. The rheological measurements were performed on swollen samples.

RESULTS AND DISCUSSION

Hydrogels based on chitosan were prepared by an easy and environmentally friendly method, using a natural monoaldehyde as chemical crosslinker, namely, salicylaldehyde (SA). By varying the initial chitosan/SA ratio, five hydrogels with various crosslinking degrees were successfully obtained according to Scheme 1 (Table 1).⁹

Structural and morphological characterization

The hydrogels were characterized by ¹H NMR spectroscopy to confirm the covalent bonding of SA to the chitosan chain *via* imine linkages. Figure 1 exemplifies the ¹H NMR spectrum for the sample C2.5, where the characteristic chemical shift of the imine proton appears as a single band at 8.37 ppm.



Scheme 1: Synthesis of chitosan hydrogels (adapted scheme⁹)

Table 1
 NH₂/CHO ratio and rheological properties of the investigated samples

Sample	NH ₂ /CHO	G' ^a (Pa)	G'' ^a (Pa)	tan δ ^a (=G''/G')	State	t _s ^b x 10 ³ (s)	E _a ^c (kJ·mol ⁻¹)	Hysteresis area (Pa·s ⁻¹)
C2	2/1	30.8	6.2	0.20	gel (G' > G'')	5.5	46.37±0.27	17417.11
C2.5	2.5/1	2.19	2.21	1.01	“critical” gel (G' ≅ G'')	476.2	34.51±9.03	3513.53
C3	3/1	0.825	1.22	1.48	“critical” gel (G' ≅ G'')	3225.8	26.07±0.04	1258.52
C3.5	3.5/1	0.294	0.866	2.95	liquid (G' < G'')	4545.5	30.90±0.06	423.00
C4	4/1	0.061	0.557	9.13	liquid (G' < G'')	-	35.97±0.05	43.83
CS ^d	-	0.078	0.860	11.02	liquid (G' < G'')	-	27.71±0.04	103.45

^a values provided from the frequency sweep measurements at 2 rad·s⁻¹ and 25 °C; ^b determined as 1/ω_S, where ω_S is the oscillatory frequency corresponding to the intersection point of G' with G'' from the frequency sweep test at 25 °C; ^c calculated from the variation of a_T as a function of 1/T-1/T_{ref} according to Eq. (1); ^d represents non-crosslinked chitosan

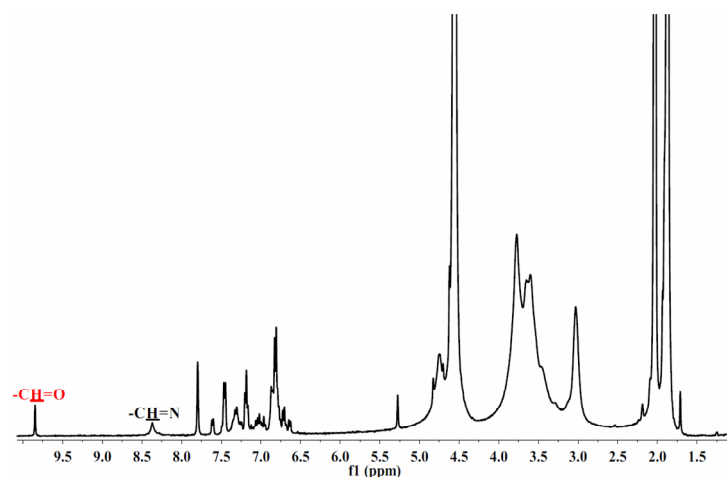


Figure 1: NMR spectra of sample C2.5

As expected, due the reversibility of imine formation in water, the chemical shift of the aldehyde proton could also be observed at 9.85 ppm in the ¹H NMR spectra. Under polarized light, chitosan displayed a birefringence texture, difficult to be ascribed, according to its semicrystalline nature (Fig. 2e). In comparison, the xerogel samples showed birefringent banded texture, characteristic of the layered supramolecular architecture of the hydrogels, a consequence of the self-assembling of the imino-chitosan derivatives to form crosslinking nodes (Fig. 2a and 2c).⁹⁻¹⁴

This was more obvious for the hydrogels with higher SA content, assumed to lead to a higher density of ordered imine clusters. The hydrogels have a super-porous morphology, correlated with the amount of salicylaldehyde used as crosslinker; in the case of the samples with a high content of the aldehyde, the morphology included interconnected pores, while those with a smaller amount revealed both pores and fibrous network (Fig. 2b and 2d). The non-crosslinked chitosan sample showed sponge-like morphology, with no well delimited pores (Fig. 2f).

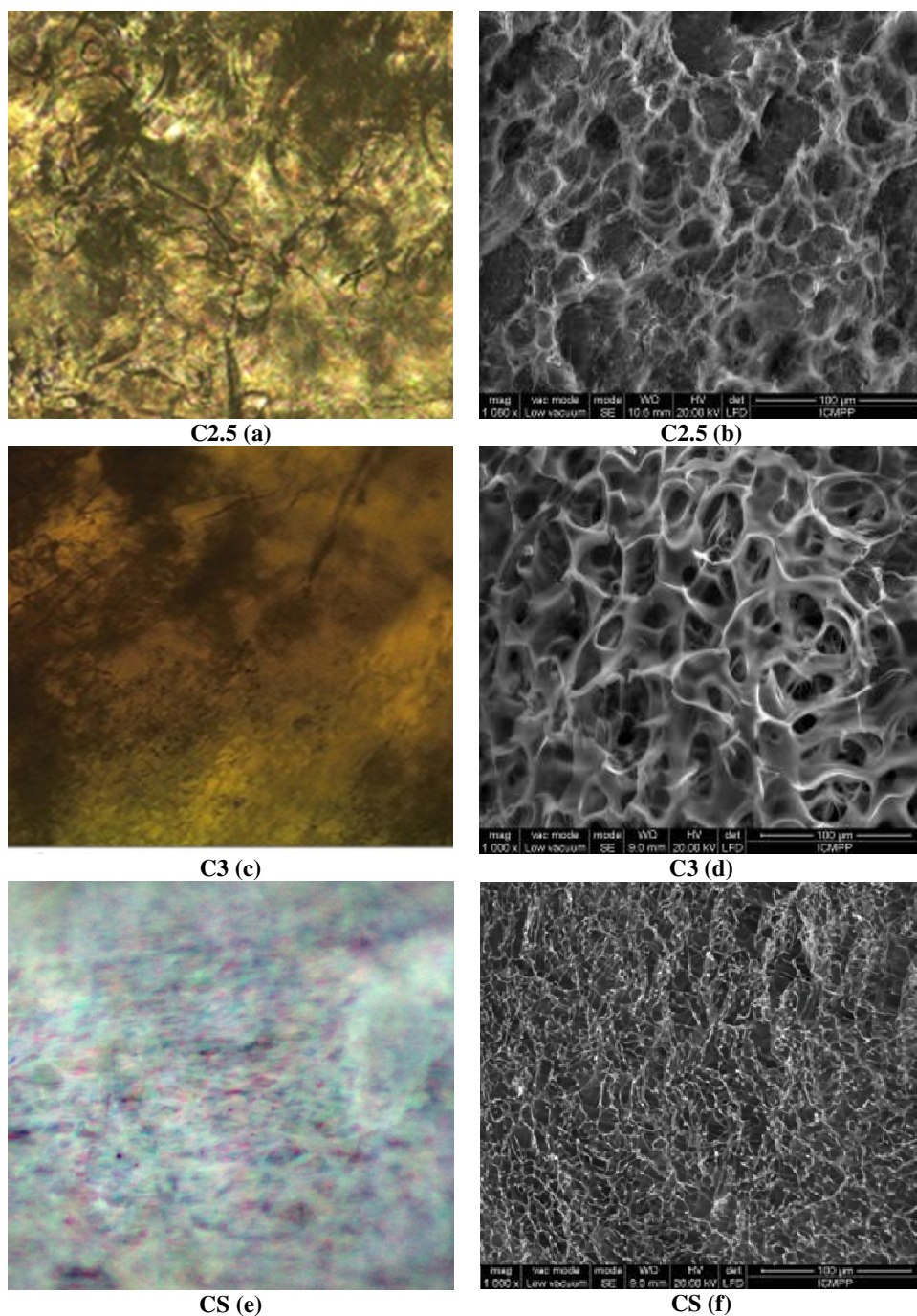


Figure 2: POM and SEM microphotographs of some representative samples (C2.5 and C3) compared to non-crosslinked chitosan sample (CS)

Rheological properties

The samples show gel- or liquid-like properties depending on the NH_2/CHO ratio. Figure 3 exemplifies the variation of viscoelastic moduli, G' and G'' , as a function of oscillatory frequency (ω) for three NH_2/CHO ratios. The values of G' , G'' and $\tan \delta (= G''/G')$, at $\omega = 2$

$\text{rad}\cdot\text{s}^{-1}$, are shown in Table 1. The increase in the SA amount (lower NH_2/CHO ratio) determines an enhancement of G' in relation to G'' . Thereby, the sample with $\text{NH}_2/\text{CHO} = 4$ exhibits liquid-like properties, while that with $\text{NH}_2/\text{CHO} = 2$ has gel-like properties. Previous studies have shown that, at 37°C , for NH_2/CHO ratios below 3.3, the

chitosan samples crosslinked with salicylaldehyde acquire gel properties.⁹ In Table 1, it can be observed that, close to NH_2/CHO ratio corresponding to the sol-gel transition, the samples acquire the behaviour characteristic of “critical” gels, with intermediate properties between solid and liquid.²⁸ For $NH_2/CHO > 3$, the samples have liquid-like properties with $G' < G''$. The samples C3.5, C4 and CS have close values for the viscoelastic parameters, G' and G'' , while $\tan \delta$ increases as the number of bridges between the chitosan chains decreases (lower amount of

salicylaldehyde) and, the physical interactions intensify.

As it is well known, for a viscoelastic fluid, in the evolution of G' and G'' as a function of ω , terminal, plateau and transition zones can be distinguished as a result of the number of interactions and the entanglements between the polymer flexible chains or, for the polymers with rigid chain, of the formed intermolecular associations.

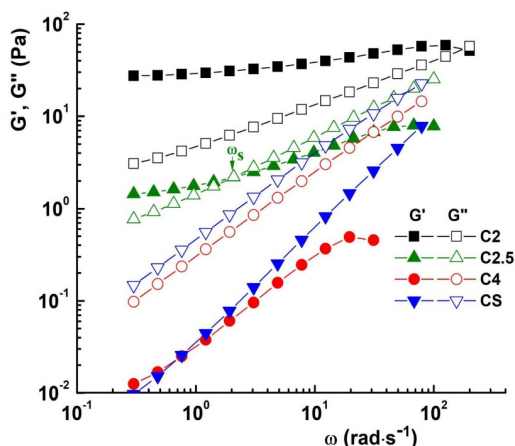


Figure 3: Variation of G' and G'' with oscillatory frequency, ω , for samples with various NH_2/CHO ratios and non-crosslinked chitosan at 25 °C

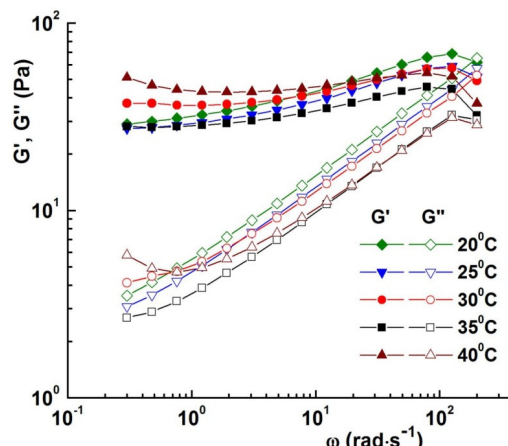


Figure 4: Variation of G' and G'' moduli of C2 at five temperatures

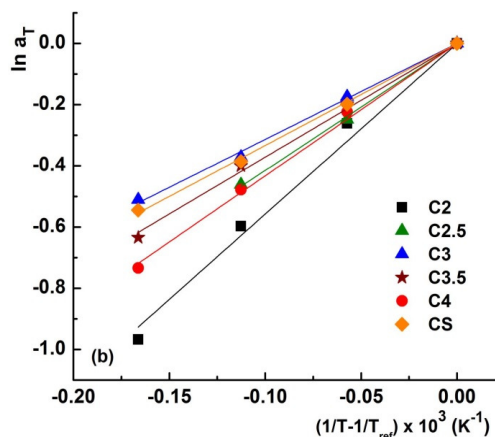
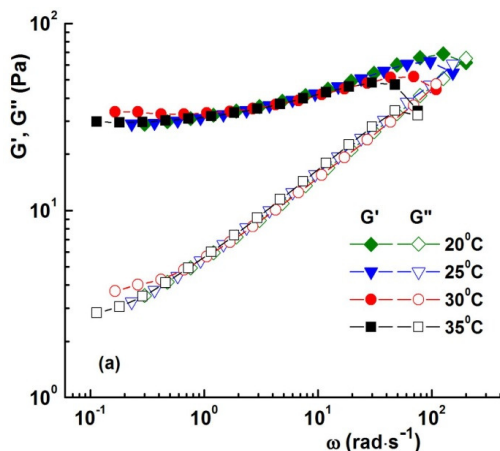


Figure 5: (a) TTSP referenced to 20 °C for C2 sample; (b) plots of $\ln(a_T)$ as a function of $(1/T-1/T_{ref})$ for investigated samples

These zones are delimited by two oscillation frequency values, where $G' = G''$, which correspond to two relaxation times defined as $t = 1/\omega$: the long-range relaxation, which delimits the

terminal and plateau zones (longest relaxation time.), $t_L = 1/\omega_L$, and the short-range relaxation, which delimits the plateau and transition zones (shortest relaxation time), $t_S = 1/\omega_S$. t_L depends on

the number of bridges between polymer chains and the strength of the network structure and t_s is given by the chain segments relaxation via bending or “breathing” motions.²⁹

For some investigated samples, the shortest relaxation time, t_s , was evidenced in the studied frequently domain (Fig. 3). The sample with $\text{NH}_2/\text{CHO} = 3.5$, characterized by a weaker network and a small amount of crosslinker, shows the highest t_s value (Table 1). t_s decreases as the density of the polymer network increases. For the sample with the smallest amount of crosslinker (sample C4), short-range relaxation was not evidenced in the studied frequency domain. Above $\text{NH}_2/\text{CHO} = 2$, t_s increases very much, suggesting a change in the interactions established in the crosslinked chitosan sample. For less crosslinked samples, the free chain segments between two crosslinking points are longer and require a longer time to relax after shearing.

Each sample was investigated by frequency sweep measurements at temperatures between 20 °C and 40 °C, and time-temperature superposition (TTSP) was performed. Figure 4 illustrates the variation of G' and G'' as a function of ω for sample C2 at five temperatures. The sample C2 exhibits gel-like properties in the frequency range of $0.3 \text{ rad}\cdot\text{s}^{-1} - 100 \text{ rad}\cdot\text{s}^{-1}$ at all investigated temperatures. For superposition, the chosen temperatures allowed only the horizontal displacement with the factor a_T , and the vertical factor b_T for the displacement was equal to 1. The data for the temperature of 40 °C (and 35 °C for C2.5) were excluded from TTSP, because this condition was not fulfilled. Figure 5a shows the experimental data of sample C2 after TTSP referenced to 20 °C. Factors a_T follow the Arrhenius equation:³⁰

$$a_T = \exp\left[\frac{E_a}{R}\left(\frac{1}{T} - \frac{1}{T_{\text{ref}}}\right)\right] \quad (1)$$

where E_a represents the activation energy for flow, R is the gas constant ($R = 8.314 \text{ J}\cdot\text{mol}^{-1}\cdot\text{K}^{-1}$) and T_{ref} is the reference temperature (20 °C).

E_a values for each sample were determined from the representation of $\ln(a_T)$ as a function of $(1/T - 1/T_{\text{ref}})$ (Fig. 5b). E_a decreases by decreasing the amount of crosslinker to the value corresponding to the gel-liquid transition ($\text{NH}_2/\text{CHO} = 3.3$) (Table 1). A further decrease in the crosslinker amount causes a slight increase of E_a , as a result of the physical interactions established, in addition to the chemical ones, between chitosan chains. The lower value of E_a for CS is probably due to the existence in the

system of only weaker physical interactions which, under shear, ensure a quick orientation of the polymer network in the flow direction.

The thixotropic properties of the investigated samples were determined by hysteresis loop measurements, which involved the increase of the shear rate, $\dot{\gamma}$, up to a maximum value of 400 s^{-1} and then its decreasing in a downward sweep (Fig. 6a).

The positive values of hysteresis areas indicate the thixotropic behaviour of the investigated samples (ascending curve over the descending one). The area between the ramps up and down gives the energy per time and volume consumed in structure breakdown. The hysteresis loop area increases from $43.83 \text{ Pa}\cdot\text{s}^{-1}$ for sample C4 to $17417.11 \text{ Pa}\cdot\text{s}^{-1}$ for sample C2. These values indicate that the samples obtained with a higher amount of crosslinker require a higher energy to break down the hydrogel structure due to the higher number of bridges between chitosan chains. In addition, for the samples with NH_2/CHO lower than 3 (higher quantity of crosslinker), the hysteresis is accompanied by a shear banding characterized by the existence of an ordered phase and a disordered one at low shear rate. The shear banding is characterized by the appearance in the flow curve of a zone where the shear stress decreases with an increasing shear rate.³¹ The width of this nonhomogeneous shear band decreases by decreasing the crosslinker amount. Correlating the degree of thixotropy with the magnitude of the hysteresis loop area, one can observe that the sample C2 exhibits the highest thixotropy degree.

The samples show shear thinning behaviour characterized by decreasing apparent viscosity, η , with an increasing shear rate, $\dot{\gamma}$ (Fig. 6b). As expected, η increases by decreasing the NH_2/CHO ratio (higher crosslinking degree). In addition, η decreases rapidly by increasing $\dot{\gamma}$ up to a shear rate value that depends on the crosslinking degree. Thereby, for the sample C2, the most pronounced decrease takes place up to about 200 s^{-1} , while, for the sample C3, η decreases more abruptly up to about 100 s^{-1} . Further increase of $\dot{\gamma}$ determines a slower decrease of η . The smallest variation in $\dot{\gamma}$ dependence of η was found for the samples C3.5, C4 and CS, characterized by lower crosslinking degree and more physical interactions between the chitosan chain segments between two junctions. The samples with $\text{NH}_2/\text{CHO} \geq 3.5$ immediately rebuild their

structure after removing the shear and return to the initial viscosity. Instead, the samples with $\text{NH}_2/\text{CHO} < 3.5$ did not completely recover after up/down sweep tests and they required longer

time to regain their viscosity (duration for the measured point was 5 s).

The thixotropic behaviour of the hydrogels was also tested with two different macroscopic approaches (Fig. 7).

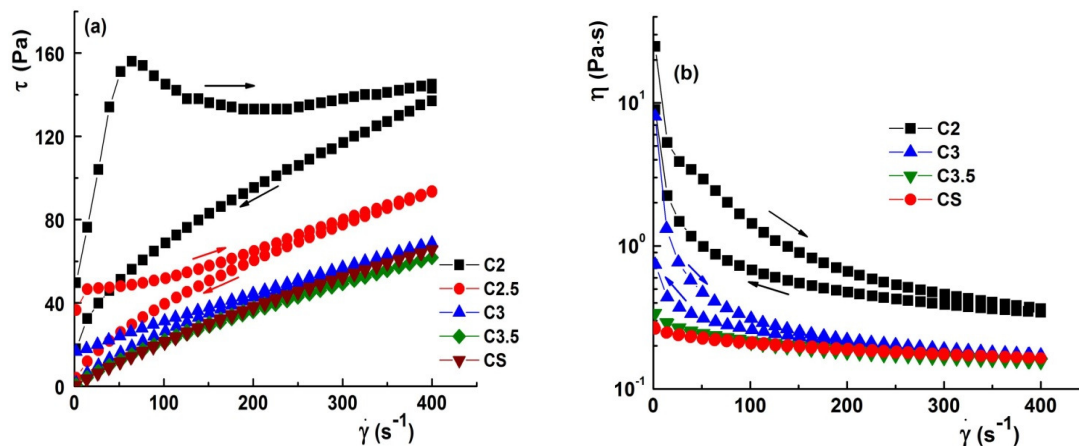


Figure 6: (a) Hysteresis loops and (b) variation of η as a function of $\dot{\gamma}$ for samples with various NH_2/CHO ratios and non-crosslinked chitosan at 25 °C

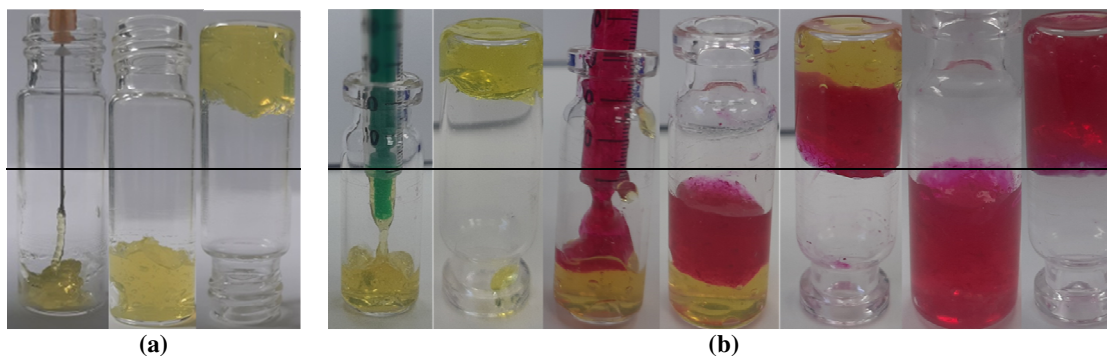


Figure 7: Self-healing macroscopic approaches using hydrogel samples, exemplified on C2

First, the hydrogels were injectable through a syringe needle and their structure was able to recover after application of this mechanical force (Fig. 7a). In the second approach, two hydrogels (one marked with Rose Bengal dye and one unmarked) were also injected through a syringe and it was observed that they stuck to each other, forming a single piece. Moreover, after being mechanically crushed, they were able to reshape into a single piece in a few seconds (Fig. 7b).

CONCLUSION

Salicyl-imine-chitosan hydrogels with rheological properties suitable for cosmetic or bio- applications were synthesized by supramolecular crosslinking of chitosan with various amounts of salicylaldehyde *via* formation of imine units and their self-assembling into

ordered clusters with the role of crosslinking nodes. The samples showed strong birefringence, in line with their supramolecular layered architecture and porous morphology observed at micrometric level. As a function of the NH_2/CHO ratio, the samples showed gel-, “critical” gel- or liquid-like behaviour. Thereby, the samples with $\text{NH}_2/\text{CHO} < 3.5$ had gel or “critical” gel properties, while the samples with higher NH_2/CHO ratio had liquid-like properties. The highest energy required to activate the flow and to break down the structure was found for the hydrogel C2, obtained with the highest crosslinker amount ($\text{NH}_2/\text{CHO} = 2$). All investigated samples showed thixotropic behaviour, characterized by positive values of the hysteresis loop area and a decrease in apparent viscosity with an increase of shear rate. The degree of thixotropy increased

with an increasing salicylaldehyde amount. The thixotropic properties of the studied salicyl-imine-chitosan hydrogels make them potential candidates for cosmetic and biomedical applications.

ACKNOWLEDGEMENTS: This research was financially supported by the Romanian National Authority for Scientific Research, CNCS-UEFISCDI, project number PN-III-P2-2.1-PED-2019-2484, contract 494 PED/2020.

REFERENCES

- ¹ I. Singha and A. Basu, *Sens. Int.*, **3**, 100168 (2022), <https://doi.org/10.1016/j.sintl.2022.100168>
- ² S. Peers, A. Montebault and C. Ladavière, *J. Control. Release*, **326**, 150 (2020), <https://doi.org/10.1016/j.jconrel.2020.06.012>
- ³ B. Qu and Y. Luo, *Int. J. Biol. Macromol.*, **152**, 437 (2020), <https://doi.org/10.1016/j.ijbiomac.2020.02.240>
- ⁴ R. Michalik and I. Wandzik, *Polymers*, **12**, 2425 (2020), <https://doi.org/10.3390/polym12102425>
- ⁵ Y. Liu, Z. Cai, L. Sheng, M. Ma, Q. Xu *et al.*, *Carbohydr. Polym.*, **215**, 348 (2019), <https://doi.org/10.1016/j.carbpol.2019.04.001>
- ⁶ M. J. Moura, M. M. Figueiredo and M. H. Gil, *Biomacromolecules*, **8**, 3823 (2007), <https://doi.org/10.1021/bm700762w>
- ⁷ M. Popa, C. Ciobanu, L. Ochiuz, J. Desbrieres and C. Peptu, *Cellulose Chem. Technol.*, **52**, 353 (2018), [https://www.cellulosechemtechnol.ro/pdf/CCT5-6\(2018\)/p.%20353-370.pdf](https://www.cellulosechemtechnol.ro/pdf/CCT5-6(2018)/p.%20353-370.pdf)
- ⁸ L. Tavares, E. E. Esparza Flores, R. C. Rodrigues, P. F. Hertz and C. P. Z. Noreña, *Food Hydrocoll.*, **106**, 105876 (2020), <https://doi.org/10.1016/j.foodhyd.2020.105876>
- ⁹ M.-M. Iftime, S. Morariu and L. Marin, *Carbohydr. Polym.*, **165**, 39 (2017), <https://doi.org/10.1016/j.carbpol.2017.02.027>
- ¹⁰ L. Marin, S. Morariu, M.-C. Popescu, A. Nicolescu, C. Zgardan *et al.*, *Chem. – Eur. J.*, **20**, 4814 (2014), <https://doi.org/10.1002/chem.201304714>
- ¹¹ D. Ailincăi, L. Marin, S. Morariu, M. Mares, A.-C. Bostanaru *et al.*, *Carbohydr. Polym.*, **152**, 306 (2016), <https://doi.org/10.1016/j.carbpol.2016.07.007>
- ¹² D. Ailincăi, I. Rosca, S. Morariu, L. Mititelu-Tartau and L. Marin, *Carbohydr. Polym.*, **276**, 118727 (2022), <https://doi.org/10.1016/j.carbpol.2021.118727>
- ¹³ A. M. Craciun, S. Morariu and L. Marin, *Polymers*, **14**, 2570 (2022), <https://doi.org/10.3390/polym14132570>
- ¹⁴ L. Marin, D. Ailincăi, S. Morariu and L. Tartau-Mititelu, *Carbohydr. Polym.*, **170**, 60 (2017), <https://doi.org/10.1016/j.carbpol.2017.04.055>
- ¹⁵ O. Guaresti, S. Basasoro, K. González, A. Eceiza and N. Gabilondo, *Eur. Polym. J.*, **119**, 376 (2019), <https://doi.org/10.1016/j.eurpolymj.2019.08.009>
- ¹⁶ A. M. Ipate, D. Serbezeanu, A. Bargan, C. Hamciuc, L. Ochiuz *et al.*, *Cellulose Chem. Technol.*, **55**, 63 (2021), <https://doi.org/10.35812/CelluloseChemTechnol.2021.55.07>
- ¹⁷ P. Sánchez-Cid, M. Jiménez-Rosado, M. Alonso-González, A. Romero and V. Perez-Puyana, *Polymers*, **13**, 2189 (2021), <https://doi.org/10.3390/polym13132189>
- ¹⁸ S. Rençber, C. N. Cheaburu-Yılmaz, F. A. Kose, S. Y. Karavana and O. Yılmaz, *Cellulose Chem. Technol.*, **53**, 655 (2019), <https://doi.org/10.35812/CelluloseChemTechnol.2019.53.64>
- ¹⁹ S. Afzal, M. Maswal and A. A. Dar, *Colloids Surf. B Biointerfaces*, **169**, 99 (2018), <https://doi.org/10.1016/j.colsurfb.2018.05.002>
- ²⁰ I. Merlusca, C. Ibanescu, C. Tuchilus, M. Danu, L. I. Atanase *et al.*, *Cellulose Chem. Technol.*, **53**, 709 (2019), <https://doi.org/10.35812/CelluloseChemTechnol.2019.53.69>
- ²¹ P. Kumar, V. Pillay and Y. E. Choonara, *Sci. Rep.*, **11**, 3104 (2021), <https://doi.org/10.1038/s41598-021-82484-x>
- ²² S. Morariu, M. Bercea and C.-E. Brunchi, *Ind. Eng. Chem. Res.*, **54**, 11475 (2015), <https://doi.org/10.1021/acs.iecr.5b03088>
- ²³ A. M. Abdel-Ghaffar, H. E.-S. Ali, M. El-Sayed and N. M. El-Sawy, *Cellulose Chem. Technol.*, **56**, 199 (2022), <https://doi.org/10.35812/CelluloseChemTechnol.2022.56.19>
- ²⁴ S. Morariu, M. Bercea and L. Sacarescu, *Ind. Eng. Chem. Res.*, **53**, 13690 (2014), <https://doi.org/10.1021/ie501891t>
- ²⁵ N. Cankaya and R. Sahin, *Cellulose Chem. Technol.*, **53**, 537 (2019), <https://doi.org/10.35812/CelluloseChemTechnol.2019.53.54>
- ²⁶ M. Bercea, E.-L. Bibire, S. Morariu, M. Teodorescu and G. Carja, *Eur. Polym. J.*, **70**, 147 (2015), <https://doi.org/10.1016/j.eurpolymj.2015.07.013>
- ²⁷ M. Bercea, E.-L. Bibire, S. Morariu and G. Carja, *Int. J. Polym. Mater. Polym. Biomater.*, **64**, 628 (2015), <https://doi.org/10.1080/00914037.2014.996712>
- ²⁸ H. H. Winter, in “Structure and Dynamics of Polymer and Colloidal Systems”, edited by R. Borsali and R. Pecola, NATO Science Series (ASIC vol. 568), Springer, Dordrecht, 2011, pp. 439–470, https://doi.org/10.1007/978-94-010-0442-8_14
- ²⁹ N. R. Agrawal, X. Yue and S. R. Raghavan, *Langmuir*, **36**, 6370 (2020), <https://doi.org/10.1021/acs.langmuir.0c00489>
- ³⁰ J. Dealy and D. Plazek, *Rheol. Bull.*, **78**, 16 (2009)
- ³¹ P. Coussot and G. Ovarlez, *Eur. Phys. J.*, **33**, 183 (2010), <https://doi.org/10.1140/epje/i2010-10660-9>